AD-A169 444 ANALYSIS OF THE DISPERSION FORCE BETWEEN A LAYERED SPHERE AND A CYLINDER(U) PRINCETON UNIV NJ DEPT OF CHEMICAL ENGINEERING D C PRIEVE ET AL. MAY 86 1/1

UNCLASSIFIED CRDEC-CR-86038 F/G 20/3 NL

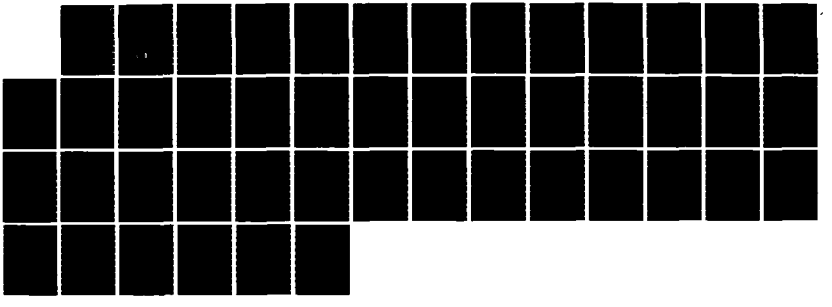

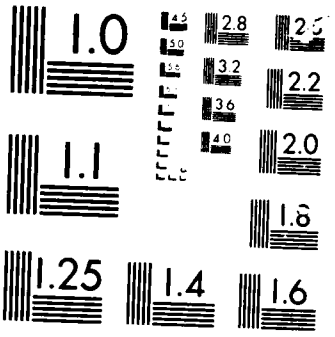
1.0
1.1
1.25
1.4
1.6
1.8
2.0
2.2
2.8
3.2
3.6
4.0
4.5
5.0
5.6

(2)

CHEMICAL RESEARCH, DEVELOPMENT & ENGINEERING CENTER

CRDEC-CR-86038

ANALYSIS OF THE DISPERSION FORCE BETWEEN A LAYERED SPHERE AND A CYLINDER

by Dennis C. Prieve
William B. Russel

DEPARTMENT OF CHEMICAL ENGINEERING
Princeton University
Princeton, New Jersey 08544

May 1986

U.S. ARMY
ARMAMENT
MUNITIONS
CHEMICAL COMMAND

Aberdeen Proving Ground, Maryland 21010-5423

Disclaimer

The findings in this report are not to be construed as an official Department of the Army position unless so designated by other authorizing documents.

Distribution Statement

Cleared for public release; distribution is unlimited.

UNCLASSIFIED
SECURITY CLASSIFICATION OF THIS PAGE

ADA 169444

REPORT DOCUMENTATION PAGE

1a. REPORT SECURITY CLASSIFICATION UNCLASSIFIED	1b. RESTRICTIVE MARKINGS
2a. SECURITY CLASSIFICATION AUTHORITY	3 DISTRIBUTION / AVAILABILITY OF REPORT Approved for public release; distribution is unlimited.
2b. DECLASSIFICATION / DOWNGRADING SCHEDULE	
4 PERFORMING ORGANIZATION REPORT NUMBER(S) CRDEC-CR-86038	5. MONITORING ORGANIZATION REPORT NUMBER(S)
6a. NAME OF PERFORMING ORGANIZATION Dept. of Chemical Engineering Princeton University 6b OFFICE SYMBOL *(If applicable)*	7a. NAME OF MONITORING ORGANIZATION U.S. Army Research Office
6c. ADDRESS *(City, State, and ZIP Code)* Princeton, NJ 08544	7b. ADDRESS *(City, State, and ZIP Code)* P.O. Box 12211 Research Triangle Park, NC 27709-2211
8a. NAME OF FUNDING / SPONSORING ORGANIZATION CRDEC 8b. OFFICE SYMBOL *(If applicable)* SMCCR-RSP-P	9. PROCUREMENT INSTRUMENT IDENTIFICATION NUMBER DO# 1284, TCN# 84-430
8c. ADDRESS *(City, State, and ZIP Code)* Aberdeen Proving Ground, MD 21010-5423	10. SOURCE OF FUNDING NUMBERS PROGRAM ELEMENT NO. / PROJECT NO. / TASK NO. / WORK UNIT ACCESSION NO.

11 TITLE *(Include Security Classification)*

Analysis of the Dispersion Force Between a Layered Sphere and a Cylinder

12 PERSONAL AUTHOR(S)
Prieve, Dennis C., and Russel, William B.

13a. TYPE OF REPORT	13b. TIME COVERED	14. DATE OF REPORT *(Year, Month, Day)*	15. PAGE COUNT
Contractor	FROM 84 Jul TO 85 Jul	1986 May	44

16. SUPPLEMENTARY NOTATION

COR: Paul D. Fedele, Ph.D., SMCCR-RSP-P, (301) 671-2262

17 COSATI CODES		
FIELD	GROUP	SUB-GROUP
20	03	
07	04	

18. SUBJECT TERMS *(Continue on reverse if necessary and identify by block number)*
Lifshitz Continuum Theory; Adhesion Forces; Dispersion Forces; Dielectric Materials; Van der Waal's Forces

19. ABSTRACT *(Continue on reverse if necessary and identify by block number)*

This report contains the analysis of and numerical results for the dispersion force between a coated cylinder and sphere based on rigorous expressions available from the Lifshitz theory for interactions between half spaces. The Derjaguin approximation satisfactorily accounts for the curvature of the bodies since the dimensions are large with respect to the relevant wavelengths. This work establishes the accuracy of a single term representation for the individual dielectric spectra and the mathematical approximations required to reduce the general expressions to relatively simple forms. In addition to providing accurate quantitative results for a variety of materials, it demonstrates that the force is always attractive for bodies interacting across a vacuum, independent of the coating, and, for those coatings which reduce the force, no optimum thickness exists.

20 DISTRIBUTION / AVAILABILITY OF ABSTRACT ☒ UNCLASSIFIED/UNLIMITED ☐ SAME AS RPT. ☐ DTIC USERS	21. ABSTRACT SECURITY CLASSIFICATION UNCLASSIFIED
22a NAME OF RESPONSIBLE INDIVIDUAL TIMOTHY E. HAMPTON	22b TELEPHONE *(Include Area Code)* (301) 671-2914 22c. OFFICE SYMBOL SMCCR-SPD-R

DD FORM 1473, 84 MAR 83 APR edition may be used until exhausted. All other editions are obsolete.

SECURITY CLASSIFICATION OF THIS PAGE
UNCLASSIFIED

PREFACE

The work described in this report was authorized under DO No. 1284 and TCN No. 84-430. Work was started in July 1984 and was completed in July 1985.

The use of trade names or manufacturer's names in this report does not constitute endorsement of any commercial products. This report may not be cited for purposes of advertisement.

This report has been approved for release to the public.

BLANK

CONTENTS

BLANK

ANALYSIS OF THE DISPERSION FORCE BETWEEN A LAYERED SPHERE AND A CYLINDER

1. INTRODUCTION

The continuum theory developed by Lifshitz and coworkers (1,2) predicts the van der Waals forces acting between colloidal or macroscopic bodies from knowledge of the dielectric spectra of the individual materials. Formal exact solutions, accounting for the effect of retardation, exist for planar geometries such as flat plates and multilayers (3) and discrete particles such as spheres and cylinders (4). Each comprises a complicated nested set of sums and/or integrals over a spectrum of wavenumbers and frequencies of the fluctuating electromagnetic modes. The power of the theory lies in the natural accommodation of the many-body effects responsible for the quantitative failure for condensed media of the pairwise additive Hamaker theory. The price is the need for complete dielectric spectra for the component materials and involved numerical calculations which obscure the relationship between these dielectric properties and the essential features of the force.

Indeed, quantitative implementation of the theory began only when Parsegian and Ninham (5,6) demonstrated that sufficiently detailed spectra could be constructed from incomplete data. Subsequently the approach has been refined (7-10) and effective Hamaker constants, defined for interactions between flat plates separated by a distance ℓ as

$$V_{fp} = -A(\ell)/12\pi\ell^2, \qquad (1.1)$$

calculated for several dozen materials. Furthermore direct measurements of forces between mica surfaces from separations of 2-100 nm (11) verify the predictions within 10-30% in vacuum and several liquids.

For nonplanar geometries results are limited. If the principle radii of curvature of the gap, R_1 and R_2, exceed substantially the wavelengths of the fluctuations (~1μm), the Derjaguin approximation,

$$V = 2\pi(R_1R_2)^{1/2} \int_h^\infty V_{fp}(\ell)d\ell, \tag{1.2}$$

is valid. Here h is the minimum separation between the surfaces. For smaller particles Mahanty and Ninham (3) suggested

$$V = - A(h)\ G(h) \tag{1.3}$$

with the effective Hamaker constant A, from the theory for flat plates, accounting for the material properties and retardation and the geometrical factor G, from the Hamaker theory, accounting for the shape effects. Pailthorpe and Russel (12) compared this approximation with the exact theory for spheres with retardation, demonstrating reasonable agreement for 0.25 and 0.50 μm polystyrene spheres in salt water. Thus there exist two reasonable and complementary approximations for interactions between particles, both based on the flat plate results.

While firmly established scientifically, the Lifshitz theory has seen limited use. Calculations of flocculation rates, phase equilibria, rheological properties, and transport coefficients generally resort to the simpler Hamaker theory, treating A as a constant parameter and, perhaps, accounting for retardation through a single characteristic wavelength. Part of the resistance arises, no doubt, from the numerical effort necessary and the uncertainty about

dielectric spectra, problems addressed squarely by Hough and White (9). An additional factor, however, is the apparent specificity of the result since spectra with multiple relaxation frequencies preclude systematic parametric studies.

Here we develop from the exact theory simple approximations, with a two-parameter representation of the dielectric spectra of the individual materials, and demonstrate them to be accurate within 20-30%. The approach preserves the principle features of the continum theory, while increasing only marginally over the Hamaker theory the numerical effort and the number of parameters required to specify the interaction potential for a particular system.

The following sections first discuss the approximate representation of the dielectric spectra (§2), which does not originate with us. Then §3 outlines the additional mathematical approximations required to reduce the rigorous results for interactions between flat plates, both non-retarded and retarded, to simple formulae and demonstrates their accuracy by comparison with exact results for several materials. §4 generalizes the treatment to coated half spaces with a similar test against evaluations of the exact expressions. Finally §5 discusses the qualitative features of the results for interaction across a vacuum showing that, although a coating can reduce the magnitude, the potential remains attractive and an optimum thickness does not exist. §6 implements the Derjaguin approximation to extend the results to interactions between a sphere and a cylinder or other curved bodies.

2. DIELECTRIC SPECTRA

The Lifshitz theory characterizes the electromagnetic fluctuations responsible for van der Waals forces in condensed media through the frequency dependent permittivity

$$\epsilon(\omega) = \epsilon'(\omega) + i\,\epsilon''(\omega) \ . \tag{2.1}$$

Hence, the dielectric spectra of the individual materials comprising a particular system must be known. Fortunately, the final mathematical form of the theory requires only $\epsilon(i\xi_n)$ with $\xi_n = 2\pi nkT/h$ $(n=0,1,\ldots)$. While the real and imaginary parts evaluated at real frequencies individually vary wildly, the complex permittivity evaluated at imaginary frequencies decreases monotonically from the static dielectric constant at n=0 to unity as n→oo. Furthermore, sampling at integral values of n emphasizes the higher frequencies, i.e. in the far infrared, the visible, and the ultraviolet beyond which the permittivities of all materials approach unity.

The representation of $\epsilon(i\xi)$ with simplified analytical forms has been discussed thoroughly by Hough and White (9). Complete representations for most materials are possible with the form

$$\epsilon(i\xi) = 1 + \sum_j d_j/(1+\xi/\omega_j) + \sum_j f_j/[1+\xi/\omega_j)^2] \ . \tag{2.2}$$

comprising a superposition of Debye dipolar relaxations and undamped resonances appropriate for relaxations in nonpolar materials. The coefficients d_j and f_j indicate the oscillator stengths, or the magnitude of the relaxation, and the ω_j the relaxation frequencies.

Hough and White (9) represented most materials by one relaxation in the infrared and a second in the ultraviolet with the parameters extracted from the static dielectric constant and data on the refractive index in the visible. For materials which do not absorb in the visible $\epsilon''=0$ and

$$\epsilon(\omega) = \epsilon'(\omega) = n^2(\omega) = 1 + f_{uv}/(1-(\omega/\omega_{uv})^2 \tag{2.3}$$

so that

$$n^2-1 = (n^2-1)(\omega/\omega_{uv})^2 + f_{uv} \ . \tag{2.4}$$

Thus $f_{uv} = \lim_{\omega\to 0} n^2 - 1 \equiv n_0^2 - 1$ and ω_{uv} follows from the slope of the plot of n^2-1 vs. $(n^2-1)\omega^2$. At zero frequency where $\epsilon''=0$ as well,

$$\epsilon(0) = 1 + f_{ir} + f_{uv} \tag{2.5}$$

giving

$$f_{ir} = \epsilon(0) - n_o^2 \ . \tag{2.6}$$

In the absence of absorption data in the infrared ω_{ir} must be specified arbitrarily, but the error should be insignificant.

Only for water, and perhaps other polar liquids, does the microwave relaxation appear significant. For some materials for which extensive data is available, such as quartz, polystyrene, and water, additional peaks in the IR and UV have been included to produce more precise spectra.

Our objective here is the simplest accurate formulation of the Lifshitz theory. To that end we retain only the single UV relaxation, evaluated as described by Hough and White (9). Thus for material j

$$\epsilon_j(i\xi_n) = 1 + (n_{oj}^2-1)/[1 + (\xi_n/\omega_j)^2], \tag{2.7}$$

providing a two parameter, n_{oj} and ω_j, characterization of any material. Values for a variety of materials are listed in Table 1.

Figure 1 compares this approximation for water with the detailed description of Gingell and Parsegian (13) based on one microwave, five infrared, and six ultraviolet relaxations. The points correspond to the latter values at the frequencies ξ_n sampled by the Lifshitz theory. Clearly the error is substantial for n=1-10 but insignificant for $n \geq 20$. Because of the complex nature of the spectra for water this should represent a worst case. In the following sections we assess the resulting error in the interaction potential.

3. UNCOATED HALF SPACES

From Lifshitz theory, the interaction energy per unit area between two uncoated half spaces, composed of materials 1 and 2, separated by thickness ℓ of material 3, is (1).

$$V_{132}(\ell) = -\frac{A_{132}(\ell)}{12\pi\ell^2} \tag{3.1}$$

where A_{132}, referred to below as the "Hamaker constant" is given by

$$A_{132} = -\frac{3}{2}kT \sum_{n=0}^{\infty}{}' \int_{r_n}^{\infty} x\{\ln[1-\Delta_{13}\Delta_{23}e^{-x}] + \ln[1-\bar{\Delta}_{13}\bar{\Delta}_{23}^{-x}]\}dx \tag{3.2}$$

$$A_{jk} = \frac{\epsilon_j s_k - \epsilon_k s_j}{\epsilon_j s_k + \epsilon_k s_j} \qquad \bar{\Delta}_{JK} + \frac{s_k - s_j}{s_k + s_j}$$

$$s_k^2 = x^2 + \left(\frac{2\xi_n \ell}{c}\right)^2 \frac{\epsilon_k - 1}{\epsilon_3} \qquad r_n = \frac{2\ell\xi_n\sqrt{\epsilon_3}}{c}$$

$$\xi_n = \frac{2\pi nkT}{h} \qquad \epsilon_k = \epsilon_k(i\xi_n)$$

with k Boltzmann's constant, T the temperature, c the speed of light in vacuum, and h Planck's constant divided by 2π. The prime (') on the sum denotes that the first term is to be multiplied by ½.

Eq. (3.2) can be simplified for extreme values of ℓ. As $\ell \to 0$, $s_k \to x$ and (3.2) becomes

$$A_{132} \sim -\frac{3}{4} kT \sum_{n=1}^{\infty}{}' \int_0^{\infty} x\{\ln[1-\Delta_{13}^0 \Delta_{23}^0 e^{-x}]\}dx \quad \Delta_{jk}^0 = \frac{\epsilon_j - \epsilon_k}{\epsilon_j + \epsilon_k} \tag{3.3}$$

In the other extreme in which $\ell \to \infty$, the lower limit of integration $r_n \to \infty$ for all n except n=0. This causes all terms in the sum of (3.2) to vanish except for the leading term leaving

$$A_{132} \sim -\frac{3}{4} kT \int_0^{x} x\{\ln[1-\Delta_{13}^0 \Delta_{23}^0 e^{-z}]\}dx \tag{3.4}$$

3.1 Approximations

Over the range of integration, the quantity $\xi_n \ell / cx$ monotonically between its maximum value of $(2\sqrt{\epsilon_3})^{-1}$ at the lower limit of integration and zero at the upper limit. Expanding in a Taylor series aobut $\xi_n \ell / cx = 0$, one obtains the following approximations:

$$s_k = x\left\{1 + 0\left[\left(\frac{\xi_n \ell}{cx}\right)^2\right]\right\} \tag{3.5a}$$

$$\Delta_{jk} = \Delta^0_{jk} + O[(\frac{\xi_n \ell}{cx})^2] \tag{3.5b}$$

$$\bar{\Delta}_{jk} = O[(\frac{\xi_n \ell}{cx})^2] \ . \tag{3.5c}$$

Approximating $\ln(1+\delta) \approx \delta$ and dropping terms of order $(\xi_n \ell/cx)^2$ allows the integrals in (3.2) to be evaluated easily. The result is

$$A_{132} \approx \frac{3}{2} kT \sum_{n=0}^{\infty}{}' \Delta^0_{13}\Delta^0_{23} (r_n+1)e^{-r_n} \ . \tag{3.6}$$

Next, we approximate the sum over n by the integral with respect to n. After expressing dn in terms of dr_n, (3.6) becomes

$$A_{132} \approx \frac{3hc}{8\pi\ell} \int_0^{\infty} \Delta^0_{13}\Delta^0_{23} (r+1)e^{-r}dr \tag{3.7}$$

where the subscript on r has been dropped. When $\epsilon_3(i\xi_n)=1$ (vacuum or rarified gas), the terms of the sum decrease monotonically with n. Then Cauchy's integral theorem provides a bound on the error made by replacing the sum by the integral

$$\left| \sum_{n=0}^{\infty}{}' s(n) - \int_0^{\infty} s(n)dn \right| \leq \frac{s(0)}{2} \tag{3.8}$$

if $0 \leq s(n+1) \leq s(n)$.

Substituting $\epsilon_3=1$ into (3.7), together with (2.7) for ϵ_1 and ϵ_2, then expressing n in terms of r and integrating, we obtain

$$A_{12} \approx \frac{3hc}{8\pi\ell} \frac{(n_{10}^2-1)(n_{20}^2-1)}{(n_{10}^2+1)(n_{20}^2+1)} r_1^2 r_2^2 \frac{F(r_1)-F(r_2)}{r_2^2 - r_1^2} \tag{3.9}$$

$$F(x) = \int_0^\infty \frac{(1+r)e^{-r}}{0r^2+x^2} dr \tag{3.10}$$

$$r_j = \frac{2\ell v_j}{c} \qquad v_j^2 = \frac{n_{j0}^2+1}{2} \omega_j^2 . \tag{3.11a,b}$$

When $r_1 = r_2$, the last factor on the right-hand-side of (3.9) is indeterminate but can be resolved as $-d^2F(x)/dx^2$. Thus, for identical half spaces, (3.9) becomes

$$A_{jj} = \frac{3hv_j}{8\pi} \frac{(n_{j0}^2-1)^2}{(n_{j0}^2+1)^2} r_j^2 F'(r_j) . \tag{3.12}$$

F(x) is a positive, monotonically decreasing function (Figure 12), which can be expressed in terms of sine and cosine integrals through their auxiliary functions, f(x) and g(x)(12):

$$F(x) = x^{-1}f(x) + g(x) \tag{3.13a}$$

$$F'(x) = x^{-1}[g(x) +1] - (x^{-2}+1)f(x) . \tag{3.13b}$$

Thus the following asymptotic behavior can be deduced:

as $x \to 0$ $\qquad F(x) \sim (\pi/2)x^{-1}$ (3.14a)

as $x \to +\alpha$ $\qquad F(x) \sim 2x^{-2}$. (3.14b)

The asympototic behavior of Eq. (3.9) as $\ell \to 0$ follows from (3.14a) as

$$A_{12} \approx \frac{3}{8} \frac{h v_1 v_2}{v_1 v_2} \frac{(n_{10}^2-1)(n_{20}^2-1)}{(n_{10}^2+1)(n_{20}^2+1)} , \tag{3.15}$$

representing the non-retarded interaction.

As a final case, consider the fully retarded interaction ($\ell \to \infty$) for which the Hamaker constant is given by (3.4), which with $\ln(1+\delta) \approx \delta$, reduces to

$$A_{132} \approx kT \frac{(\epsilon_{01}-\epsilon_{03})(\epsilon_{02}-\epsilon_{03})}{(\epsilon_{01}+\epsilon_{03})(\epsilon_{02}+\epsilon_{03})} . \tag{3.16}$$

In obtaining (3.16), no assumption was made concerning the dielectric relaxation of the materials. Thus ϵ_{oj} denotes the true zero-frequency dielectric constant, whereas the n_{jo} in (3.9), (3.12) and (3.15) corresponds to the zero-frequency dielectric constant computed from the UV absorption peak only.

3.2 Testing of Approximations

Using tabulated data (7), we evaluated the non-retarded Hamaker constant from (3.15) and compared the result to that from (3.9) with $\ell=0$ and $\epsilon_3=1$, using IR and (in the case of water) microwave absorption peaks. The results for identical halfspaces are given in Table 1 while those for dissimilar halfspaces are given in Table 2.

Considering the simplicity of (3.15), its accuracy in the above tests is remarkable. Especially so are the cases involving water which absorbs strongly in the microwave frequency range. Eq. (3.15) only uses data on the UV absorption peak, which accounts for only 10% of the dielectric relaxation for water.

Except for the case of quartz/polystyrene, all of the Hamaker constants in the column labelled "Eq. 3.9" of Tables 1 and 2 were also calculated by Hough and White (7). Our values agree closely with theirs.

Fig.2 compares Hamaker constants computed from the full series given by (3.2) to those from the approximate analytical expressions developed above, over the entire spectrum of separation distance. Eq. (3.12) clearly provided a reasonable approximation at small to moderate separations, but begins to diverge from (3.2) for separations larger than one micron. Also note the (3.16) predicts that A asymptotes to a constant as $\ell \to \infty$, whereas (3.9) or (3.12) incorrectly predicts that A is $O(\ell^{-1})$. This divergence in asymptotic behavior arises from replacing the sum by the integral, which introduces an uncertainty equal to half of the leading term. Although the leading term is a small fraction of the sum for small to moderate ℓ, only it survives as $\ell \to \infty$. Like Table 1, Fig. 2 shows (3.15) to be a good approximation for the non-retarded limit. Also (3.16), with the true zero-frequency dielectric constants represents well the fuly retarded limit.

Fig. 3 shows the same comparisons for two dissimilar half spaces. Water was chosen for the second half space because absorption in the UV, the only factor considered in (3.9), accounts for only 10% of the total dielectric relaxation. Thus water represents the worst case. Despite this, the agreement is as good as in Fig. 2.

Figs. 4 and 5 show the effect of UV absorption frequency, ω_j, and UV absorption peak height, n_{jo}^2-1, on the Hamaker constant computed from (3.12). A large peak at high frequency gives rise to the strongest attraction. Increasing the peak height increases the Hamaker constant at all separations by about the

same fraction, whereas increasing the absorption frequency increases the Hamaker constant at small separations by a larger fraction than at large separations. Note that the reduction in the Hamaker constant due to retardation becomes noticeable when the separation is larger than about 2nm.

Fig. 6 gives the non-retarded Hamaker constant for an arbitrary set of physical properties and illustrates the results with a number of common materials. Teflon, water, and short-chain alkanes give the smallest Hamaker constant, quartz and sapphire the largest.

4. COATED HALF SPACES

The effective Hamaker constant for the interaction between two half spaces, one composed of material 1 with a coating of thickness b of material 4 and the other of pure 2, separated by a distance ℓ filled with gas(vacuum) is (1, p. 143)

$$A_{142} = -\frac{3}{2} kT \sum_{n=0}^{\infty} \int_{r_n}^{\infty} x\{\ln[1-\Delta_{31}\Delta_{32}\exp(-x)] + \ln[1-\bar{\Delta}_{31}\bar{\Delta}_{32}\exp(-x)]\}dx \tag{4.1}$$

with

$$\Delta_{31} = \{\Delta_{34} + \Delta_{41}\exp(-r_n bs_4/\ell)\}/\{1+\Delta_{34}\Delta_{41}\exp(-r_n bs_4/\ell)\} \tag{4.2}$$

and Δ_{34}, Δ_{41}, Δ_{32}, $\bar{\Delta}_{34}$, $\bar{\Delta}_{41}$, $\bar{\Delta}_{32}$, s_j, ϵ_j, r_n, and $\S \to \S_n$ defined as in (3.2). The limiting forms of the effective Hamaker constant,

$$A_{142}(\ell) \to A_{12}(\ell) \quad \text{as } \ell \to \infty$$
$$\to -A_{42}(\ell) \quad \text{as } \ell \to 0 \tag{4.3}$$

indicate that the coating completely masks the substrate at small separations but becomes invisible for separations large with respect to its thickness.

Applications of the approximations outlined and tested in §3 leads to a substantially simplified form of (4.1). The expansion about $\xi_n \ell/cx=0$ yields

$$\Delta_{31} = \{\Delta_{34} + \Delta_{41}\exp(-bx/\ell)\}/\{1+\Delta_{34}\Delta_{41}\exp(-bx/\ell)\} \tag{4.4}$$

together with (3.5a-c).

Then expanding the logarithms and truncating the series at $O(\Delta^2)$ permits an analytic integration over x such that

$$A_{142} = \frac{3}{2} kT \sum_{n=0}^{\infty} \{(1-\epsilon_4)/(1+\epsilon_4)(1+r_n)\exp(-r_n) + (\epsilon_4-\epsilon_1)/(\epsilon_4+\epsilon_1)$$

$$[1+(1+b/\ell)r_n]/(1+b/\ell)^2\exp-(1+b/\ell)r_n\}(1-\epsilon_2)/(1+\epsilon_2). \tag{4.5}$$

The conversion of the sum over n to an integral and substitution of the single term approximations for the dielectric spectra provides an expression which is integrable via a partial fraction expansion. The final result

$$A_{142} = \frac{3hc}{8\pi\ell} \frac{n_{20}^2-1}{n_{20}^2+1} \{\frac{n_{40}^2-1}{n_{40}^2+1} \frac{r_2^2 r_4^2}{r_2^2-r_4^2} (F(r_4) - F(r_2))$$

$$+ \frac{n_{10}^2-n_{40}^2}{n_{10}^2+n_{40}^2} \frac{r_2^2\rho_1^2\rho_4^2}{1+b/\ell} [\frac{1 - r_2^2/r_{14}^2}{r_2^2-\rho_1^2)(r_2^2-\rho_4^2)} F(r_2(1+b/\ell))$$

(4.6)

$$+ \frac{1 - \rho_1^2/r_{14}^2}{(\rho_1^2 - \rho_4^2)(\rho_1^2 - r_2^2)} F(\rho_1(1+b/\ell))$$

$$+ \frac{1 - \rho_4^2/r_{14}^2}{(\rho_4^2 - \rho_1^2)(\rho_4^2 - r_2^2)} F(\rho_4(1+b/\ell))]]$$

involves the function F defined by (3.10) and

$$\rho_{1,4}^2 = \frac{1}{2}(r_1^2 + r_4^2)\{1 \pm [1-8 \frac{n_{40}^2 + n_{10}^2}{(n_{40}^2+1)(n_{10}^2+1)} \frac{r_1^2 r_4^2}{(r_1^2+r_4^2)^2}]^{1/2} \tag{4.7}$$

$$\frac{1}{r_{14}^2} = \frac{n_{40}^2 - 1}{n_{40}^2 - n_{10}^2} \frac{n_{10}^2 + 1}{2r_1^2} + \frac{n_{10}^2 - 1}{n_{10}^2 - n_{40}^2} \frac{n_{40}^2 + 1}{2r_4^2} .$$

The limits for b-0 or $n_4^2 \to 1$ reduce to the previous result (3.9).

Although A_{142} is more complex than A_{12}, both require only the numerical evaluation of F(x). The potential, of course, now depends on the n_{0i} and ω_i for each of the three materials plus b and ℓ. Since the character of the functions is not changed by the layer, the approximations should be as accurate as for the uncoated case.

5. CONSEQUENCES OF COATING

5.1 Coated Half Spaces Always Attract Across a Vacuum

One reason for coating a surface is to alter its interaction with other surfaces. In general, the coating can reverse the sign of the interaction (for example, convert an attractive interaction into a repulsive one). However, the interaction between two half spaces separated by vacuum is always attractive, whether or not the surfaces are coated. The proof follows.

When $\epsilon_3 = 1$, the definitions below (3.20) yield

$$s_j^2 = x^2 + (\epsilon_j - 1)r_n^2 \tag{5.1}$$

$$\Delta_{j3} = \frac{\epsilon_j x - s_j}{\epsilon_j x + s_j} \qquad \bar{\Delta}_{j3} = \frac{s_j - x}{s_j + x} \tag{5.2a,b}$$

Lemma 1: $\epsilon_j x \geq s_j$ For $\epsilon_j \geq 1$, $s_j \geq 0$, and $x \geq 0$, the proof follows from (5.1):

$$(\epsilon_j x)^2 - s_j^2 = (\epsilon_j - 1)[(\epsilon_j + 1)x^2 - r_n^2] \geq (\epsilon_j + 1)x^2 - r_n^2 \geq x^2 - r_n^2 \geq 0. \tag{5.3}$$

This last inequality results from the definition of x as a dummy variable of integration (see (3.2) which spans the interval $r_n \leq x \leq \infty$.

Lemma 2: $\Delta_{j3} \geq 0$ The proof follows directly from (5.2a) and Lemma 1.

Lemma 3: $\Delta_{k3} \geq \Delta_{kj}$ Using the definition following (3.2), this inequality is equivalent to

$$\frac{\frac{\epsilon_k x}{s_k} - 1}{\frac{\epsilon_k x}{s_k} + 1} \geq \frac{\frac{\epsilon_k s_j}{\epsilon_j s_k} - 1}{\frac{\epsilon_k s_j}{\epsilon_j s_k} + 1} \quad . \tag{5.4}$$

Both sides of this inequality have the form (y-1)/(y+1), which is a monotonically increasing function of y; thus the proof requires only that

$$\frac{\epsilon_k x}{s_k} \geq \frac{\epsilon_k s_j}{\epsilon_j s_k} \tag{5.5}$$

which is implied by Lemma 1.

Lemma 4: $\Delta_{j3}(b_k) \geq 0$ Since $|\Delta_{j3}|$, $|\Delta_{jk}|$, and the exponential factor in (4.7) are all less than unity, their product must be less than unity in absolute value. Thus the denominator of (4.1) is positive, regardless of the sign of Δ_{jk}, and the sign of $\Delta_{j3}(b_k)$ is determined by the numerator. Lemmas 2 and 3 imply

$$e^{z}\Delta_{k3} \geq \Delta_{k3} \geq \Delta_{kj} = -\Delta_{jk} \tag{5.6}$$

and

$$\Delta_{k3} + \Delta_{jk}e^{-z} \geq 0$$

provided $z \geq 0$. Thus the numerator of (4.2) is positive. The corollaries to Lemmas 2-4 for the Δ can be similarly proven using $s_j \geq k$ instead of Lemma 1 and (5.2b) instead of (5.2a).

From Lemmas 2 and 4 and their corollaries, it follows that, when the two (coated) halfspaces are separated by vacuum, all the Δ's appearing in (4.1) are positive numbers. Thus, the logarithms are negative and the net interaction is attractive, regardless of the properties of any films or of the substrates. Coating of the halfspace by a film cannot make the interaction repulsive.

5.2 Effect of Film Thickness

Although coating one or both of the half spaces cannot change the sign of the interaction across a vacuum, the coating can alter the magnitude of the interaction. Figure 7 shows the effect of film thickness on the interaction of

two quartz half-spaces with one coated with a film of polystyrene. When the nonretarded Hamaker constant for coating/vacuum/substrate is less than that for substrate/vacuum/substrate, the former Hamaker constant can exhibit a maximum with respect to separation distance, ℓ. However, this maximum disappears when the Hamaker constant is divided by ℓ^2 to obtain the interaction energy (3.1). Indeed, film thickness, b, primarily determines the separation distance at which the material properties of the substrate (1) and the coating (4) contribute equally to the interaction with the other half space (2), i.e., at $\ell \approx 3b$

$$2A_{1(4)2}(\ell) \approx A_{12}(\ell) + A_{42}(\ell).$$

Thus the thicker the coating, the greater the range of separation distance over which the coating's properties mask those of the substrate.

5.3 Absence of an Optimum Coating Thickness

While a suitable coating will reduce the attraction between two substrates, there exists no optimum thickness, i.e., the attraction at any fixed separation ℓ varies monotonically with increasing b. To demonstrate this we evaluate $\partial A_{142}/\partial b$ and rearrange the result into

$$\frac{\partial A_{142}}{\partial b} = - \frac{\int_0^\infty (1+r)e^{-r}R(b/\ell)dr}{(r_2^2-\rho_1^2)(r_2^2-\rho_4^2)(\rho_1^2-\rho_4^2)} \qquad (5.7)$$

with

$$R(b/\ell) = 2\frac{r^4}{r_{14}^2}(1+b/\ell)^2\left[1+\left(\frac{r_{14}}{r}\right)^2(1+b/\ell)^2\right] \quad x \tag{5.8}$$

$$\frac{r_2^4(\rho_4^2-\rho_1^2) + \rho_1^4(r_2^2-\rho_4^2) + \rho_4^4(\rho_1^2-r_2^2)}{[r^2+r_2^2(1+b/\ell)^2]^2\,[r^2+\rho_1^2(1+b/\ell)^2]^2[r^2+\rho_4^2(1+b/\ell)^2]^2} .$$

Thus the dielectric properties determine the sign of the derivative with no value of b/ℓ for which $\partial A_{124}/\partial b = 0$. In the absence of other constraints no optimum exists.

5.4 Effect of Coating's Physical Properties

Figs. 8 and 9 show the effect of absorption strength and frequency of the coating on the interaction of two quartz half spaces across vacuum. The addition of the coating can either increase or decrease the attraction. Since the curves rarely intersect one another, a ranking of various coating materials with respect to their effect on the interaction could be based on the Hamaker constant evaluated at just one separation distance, say ℓ=0. At ℓ=0, the Hamaker constant for substrate/coating/vacuum/substrate is identical to that for a half space of the opposing substrate and can be estimated from (3.15).

As an example, Fig. 10 indicates a ranking of various potential materials for coating one of two interacting quartz half-spaces. Coatings of materials above the curve passing through quartz will strengthen the attraction, while those materials below the curve will weaken it. Materials closest to the lower left corner of this plot (weak UV absorption in low frequency end of the UV

spectrum) will reduce the interaction most. Of those materials listed, Teflon seems best, with water and short-chain alkanes next. However, none of the materials listed will reduce the interaction between two quartz half spaces by more than 50%.

To show that rankings based on calculations of the nonretarded Hamaker constant at ℓ=0 are approximately applicable at other separations, we computed the profile with separation distance for four different materials, two with a nonretarded A of 5×10^{-20}J and two with 8×10^{-20}J. The material properties were chosen from Fig. 10 to be as different as possible. Yet the curves in each pair (Fig. 11) nearly coincide at all separations.

6. INTERACTIONS BETWEEN A SPHERE AND A CYLINDER

The expressions developed in the previous sections for the interaction potential between uncoated and coated half spaces can be transformed into interactions between a sphere of radius a and a cylinder of radius R through (1.2) with R_1=a and R_2=aR/(a+R). The approximation requires only that the principle radii of curvature exceed significantly the minimum separation h and the maximum significant wavelength $L=2\pi c/\omega\sim1\mu m$,

Substitution of (4.6) for the coated systems leads to

$$V = -\frac{hc}{32\pi}\,\frac{a}{h(1+a/R)^{1/2}}\,\frac{n_{20}^2-1}{n_{20}^2+1}\left\{\frac{n_{40}^2-1}{n_{40}^2+1}\,\frac{r_2^2r_4^2}{r_2^2-r_4^2}\left(\frac{G(r_4)}{r_4}-\frac{G(r_2)}{r_2}\right)\right.$$

$$\left. + \frac{n_{10}^2-n_{40}^2}{n_{10}^2+n_{40}^2}\,r_2^2\rho_2^2\rho_4^2\left[\frac{1-r_2^2/r_{14}^2}{(r_2^2-\rho_1^2)(r_2^2-\rho_4^2)}\,\frac{G(r_2(1+b/h))}{r_2}\right.\right. \qquad (6.1)$$

$$+ \frac{1-\rho_1^2/r_{14}^2}{(\rho_1^2-\rho_4^2)(\rho_1^2-r_2^2)} \frac{G(\rho_1(1+b/h))}{\rho_1} + \frac{1-\rho_4^2/r_{14}^2}{(\rho_4^2-\rho_1^2)(\rho_4^2-r_2^2)} \frac{G(\rho_4(1+b/h))}{\rho_4}]] \ .$$

These expressions require the numerical evaluation of

$$G(x) = \int_0^\infty \ln(1+(r/x)^2(1+r)\exp(-r)/r^2 dr \tag{6.2}$$

which has limiting forms

$$r \to \infty \qquad G \sim 2/x^2$$

$$r \to 0 \qquad G \sim O(1/x) \ . \tag{6.3}$$

We have performed no numerical calculations since the potentials should behave similarly to those for flat plates and the force follows directly from the flat plate potential as

$$F = -\partial V/\partial h = 2\pi(R_1R_2)^{1/2} V_{fp}(h) \ . \tag{6.4}$$

Hence the magnitude of the force for a coated system can be calculated directly from (4.6) and (6.4) for comparison with gravitational or viscous forces which might be important in a specific application.

REFERENCES

1. E. M. Lifshitz, J. Exp. Theoret. Phys. USSR 29, 94(1955).

2. I. E. Dzaloshinskii, E. M. Lifshitz and L. P. Pitaerskii, Adv. Phys. 10 165(1961).

3. J. Mahanty and B. W. Ninham, Dispersion Forces, Academic Press 1976.

4. D. Langbein, Theory of van der Waals Attraction, Springer Tracts in Modern Physics, Springer-Verlag 1974.

5. V. A. Parsegian and B. W. Ninham, Nature (London) 227 739(1969).

6. B. W. Ninham, and V. A. Parsegian, Biophys. J. 10 646(1970).

7. V. A. Parsegian, "Long Range van der Waals Forces" in Physical Chemistry: Enriching Topics in Colloid and Surface Science (ed. H. van Olphen and K. J. Mysels) Theorex, 1975, pp. 27-72.

8. D. Y. C. Chan and P. Richmond, Proc. Roy. Soc. Lond. A 353 163(1977).

9. D. B. Hough and L. R. White, Adv. Colloid Inter. Sci. 14 3(1980).

10. V. A. Parsegian and G. H. Weiss, J. Colloid Inter. Sci 81 285(1981).

11. J. N. Israelachvili, Intermolecular and Surface Forces, Academic Press 1985.

12 B. A. Pailthorpe and W. B. Russel, J. Colloid Inter. Sci. 89 563(1982).

13. D. Gingell and V. A. Parsegian, J. Theor. Biol. 36 41(1972).

14. M. Abramowitz and I. A. Stegun, Handbook of Mathematical Functions, Dept. of Commerce, Washington, DC, 1970.

BLANK

APPENDIX A: TABLES

TABLE 1

Non-Retarded Hamaker Constants

Identical Half-Spaces Across Vacuum

Material	ω_j	n_{jo}^2-1	A_{jj} (10^{-13}erg)	
	($10^{16}s^{-1}$)		Eq. 3.9	Eq. 3.3
Quartz	2.032	1.359	8.52	8.83
Polystyrene	1.354	1.447	6.19	6.37
Sapphire	2.017	2.071	14.72	15.6
Teflon	1.566	0.748	2.69	2.75
Water	1.899	0.755	3.51	3.90

TABLE 2

Non-Retarded Hamaker Constants
Dissimilar Half-Spaces Across Vacuum

Materials(j/k)	A_{jk} (10^{-13} erg)	
	Eq. 3.15	Eq. 3.3
Quartz/Water	5.31	5.59
Sapphire/Water	6.92	7.40
Quartz/Polystyrene	7.16	7.34

APPENDIX B: FIGURES

FIGURE CAPTIONS

1. Dielectric spectrum for water from the approximation 2.7 (----) compared with the detailed construction of Gingell and Parsegian (13) evaluated at the sampling frequencies $\xi_n(X)$.

2. Interaction of identical quartz half spaces across vacuum. Test of approximations (----) against full series solution (X) given by (3.2).

3. Interaction of quartz and water across vacuum. Test of approximations (----) against full series soution (X) given by (3.2).

4. Effect of strength of UV absorption strength on the interaction of two identical uncoated half spaces across vacuum, as computed from (3.12). From bottom to top, n_{10}^2-1 = 0.5, 1, 1.5, 2, and 2.5 while $\omega = 1.5\times10^{16}$ Hz.

5. Effect of UV absorption frequency on the interaction of two identical uncoated half spaces across vacuum, as computed from (3.12). From bottom to top, ω = 1, 1.25, 1.5, 1.75, 2, and 2.25×10^{16} Hz while $n_{10}^2-1 = 1.5$

6. Effect of UV absorption strength and frequency on the nonretarded interaction of two identical uncoated half spaces across vacuum. Curves denote loci of A_{jj}=const, computed from (3.15), while points denote properties of particular materials (9). From lower left to upper right, A_{jj} = 2, 3, 4 ...11×10^{-20}J.

7. Effect of film thickness on the interaction of two quartz half-spaces separated by vacuum when one half space is coated with a film of

polystyrene. Film thickness increases from upper to lower curves: b = 0, 0.1, 0.316, 1, 3.16, 10nm. Lower curve represents a polystyrene half space interacting with a quartz half space.

8. Effect of absorption strength of coating upon the interaction of two quartz half spaces across vacuum when one of the half spaces is coated. From bottom to top, n_{40}^2-1 = 0.001, 0.5, 1, 1.5, 2, 2.5. Other properties of film include b = 1nm, $\omega_4 = 1.354 \times 10^{16} s^{-1}$.

9. Effect of absorption frequency of coating upon the interaction of two quartz half spaces across vacuum when one of the half spaces is coated. From bottom to top, ω_4 = 0.5, 1, 1.5, 2, 2.5×10^{-16} Hz. Other properties of film include b = 1nm, $n_{40}^2-1 = 0.447$.

10. Screening of potential coating materials. Curves give the value of the nonretarded Hamaker constant for interaction across vacuum of a half space with the properties given by the ordinate and abscissa with a second half space of quartz, as computed from (3.15). From lower left to upper right, A_{jk} = 4, 5, 6 ... 11 x 10^{-20}J.

11. A test of the hypothesis that Fig. 10 is adequate for screening potential materials for coating one of two quartz half spaces interacting across vacuum. The four curves correspond to four different 1nm coatings, two with properties at opposite ends of the 5 x 10^{-20}J line in Fig. 10 and two at opposite ends of the 8×10^{-20}J line.

12. Plot of F(x) obtained by numerical integration on (3.10).

Fig. 1

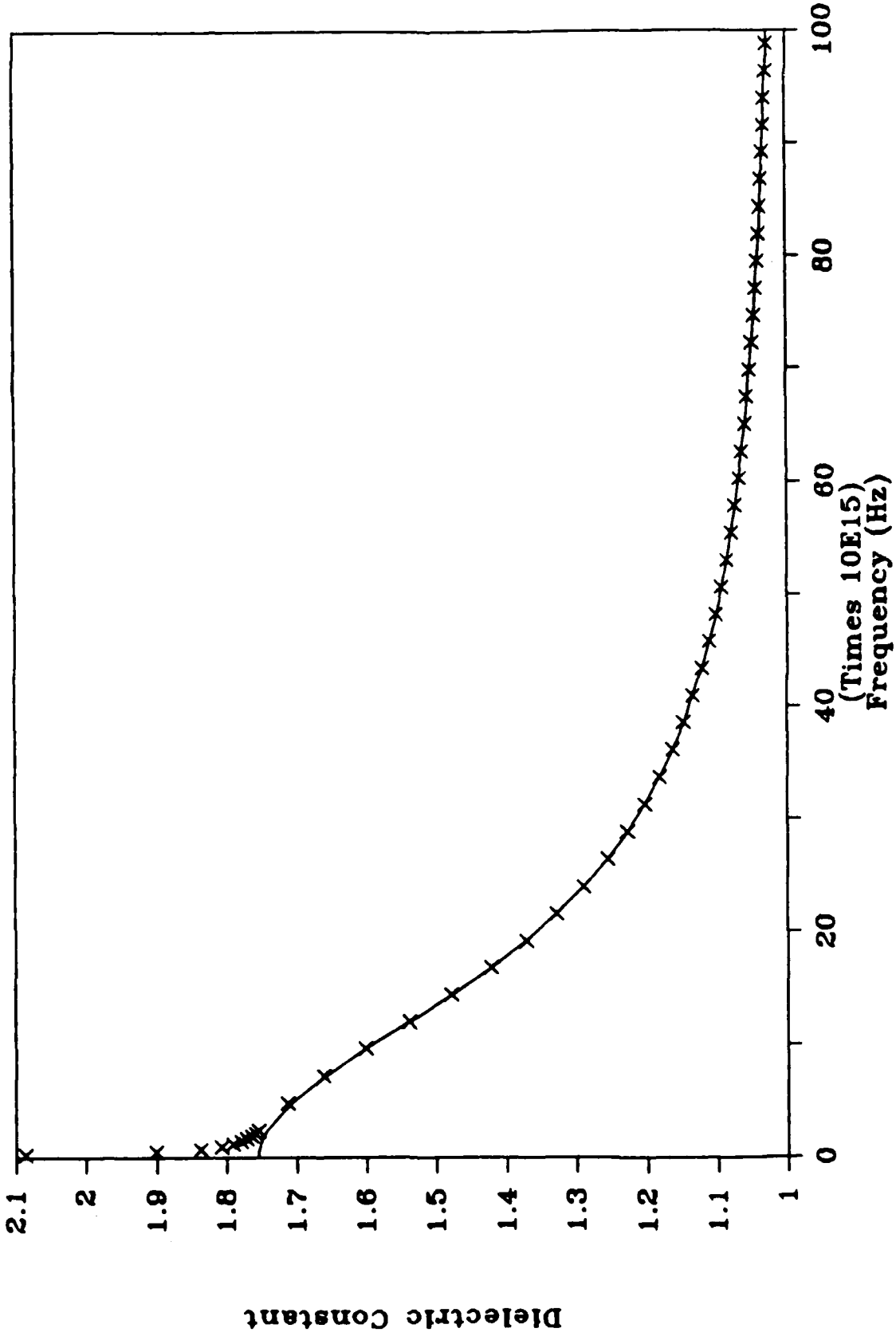
Dielectric Constant
2.1
2
1.9
1.8
1.7
1.6
1.5
1.4
1.3
1.2
1.1
1
0
20
40
60
80
100
(Times 10E15)
Frequency (Hz)

Fig. 2

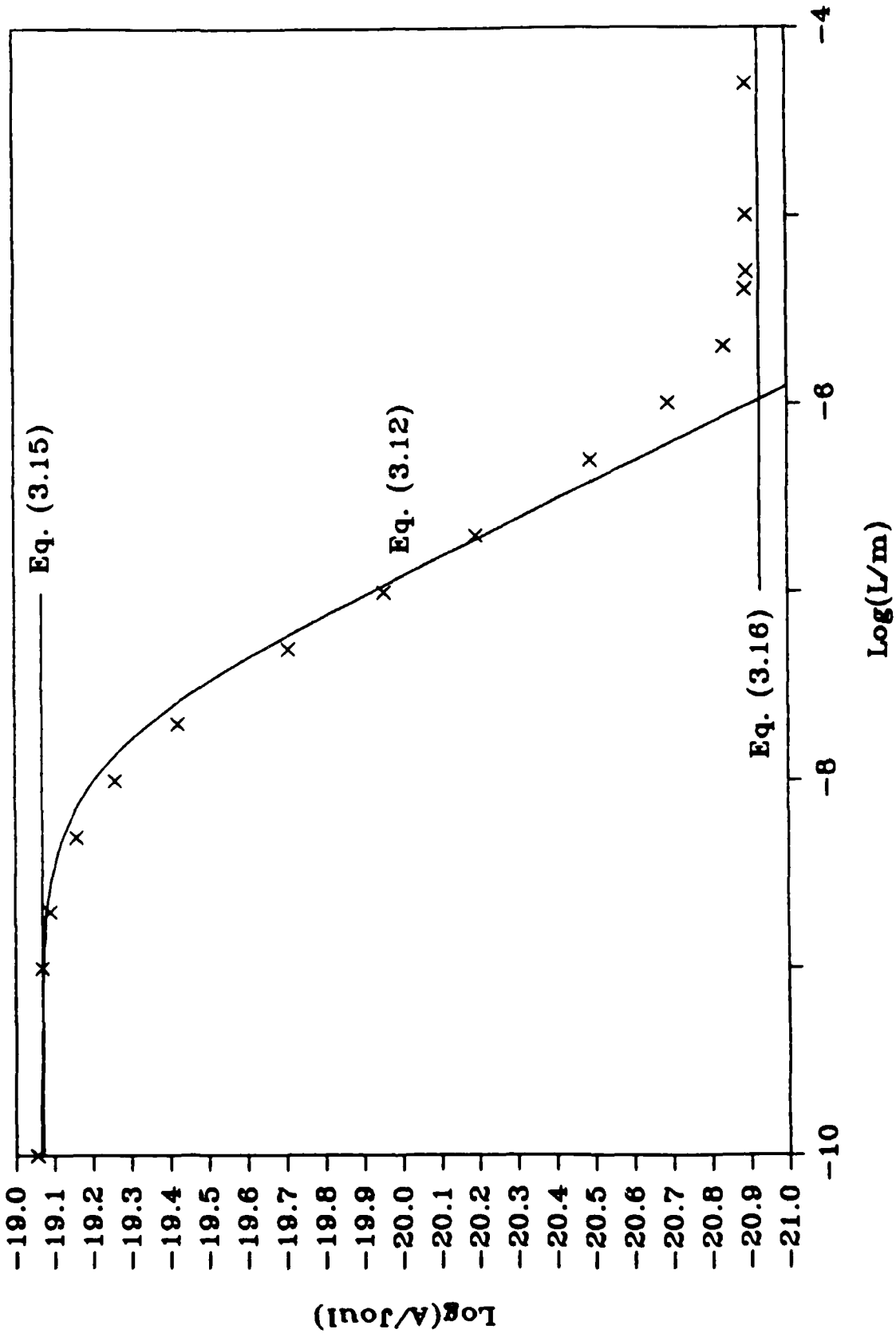
Eq. (3.15)
Eq. (3.12)
Eq. (3.16)
Log(A/Joul)
Log(L/m)
-19.0
-19.1
-19.2
-19.3
-19.4
-19.5
-19.6
-19.7
-19.8
-19.9
-20.0
-20.1
-20.2
-20.3
-20.4
-20.5
-20.6
-20.7
-20.8
-20.9
-21.0
-4
-6
-8
-10

Fig. 3

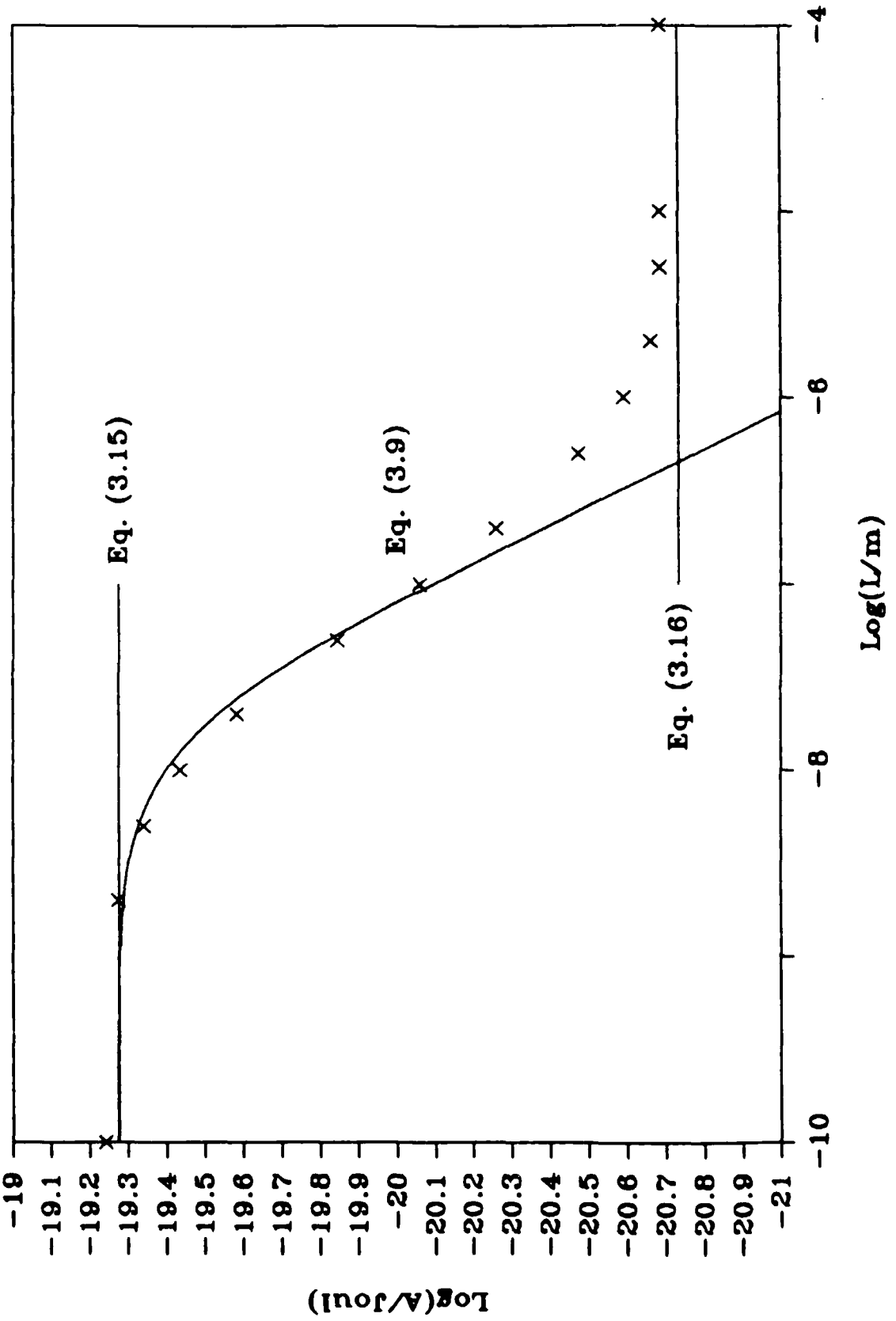
Eq. (3.15)
Eq. (3.9)
Eq. (3.16)
Log(A/Joul)
Log(L/m)
-19
-19.1
-19.2
-19.3
-19.4
-19.5
-19.6
-19.7
-19.8
-19.9
-20
-20.1
-20.2
-20.3
-20.4
-20.5
-20.6
-20.7
-20.8
-20.9
-21
-4
-8
-8
-10

Fig. 4

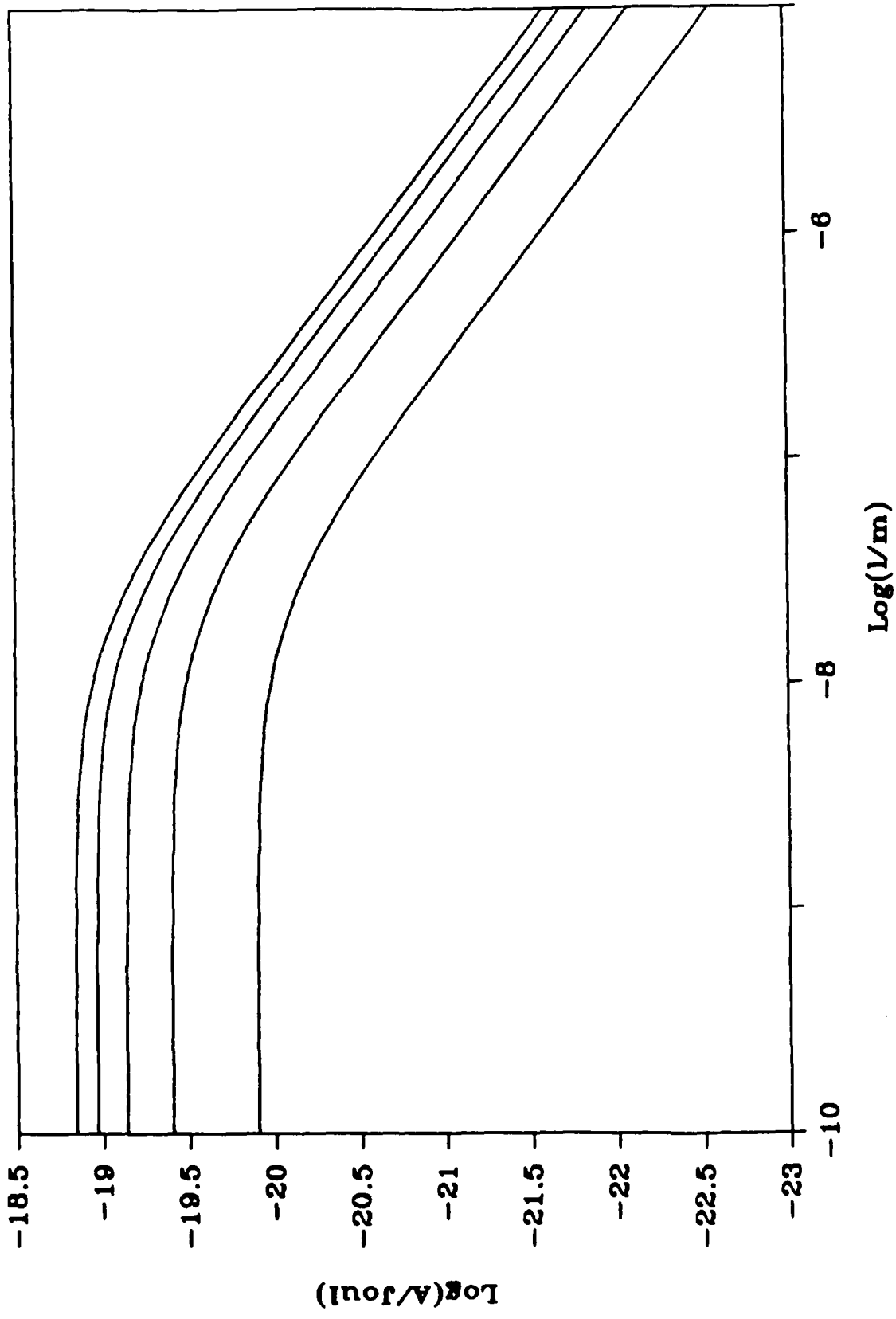

Fig. 5

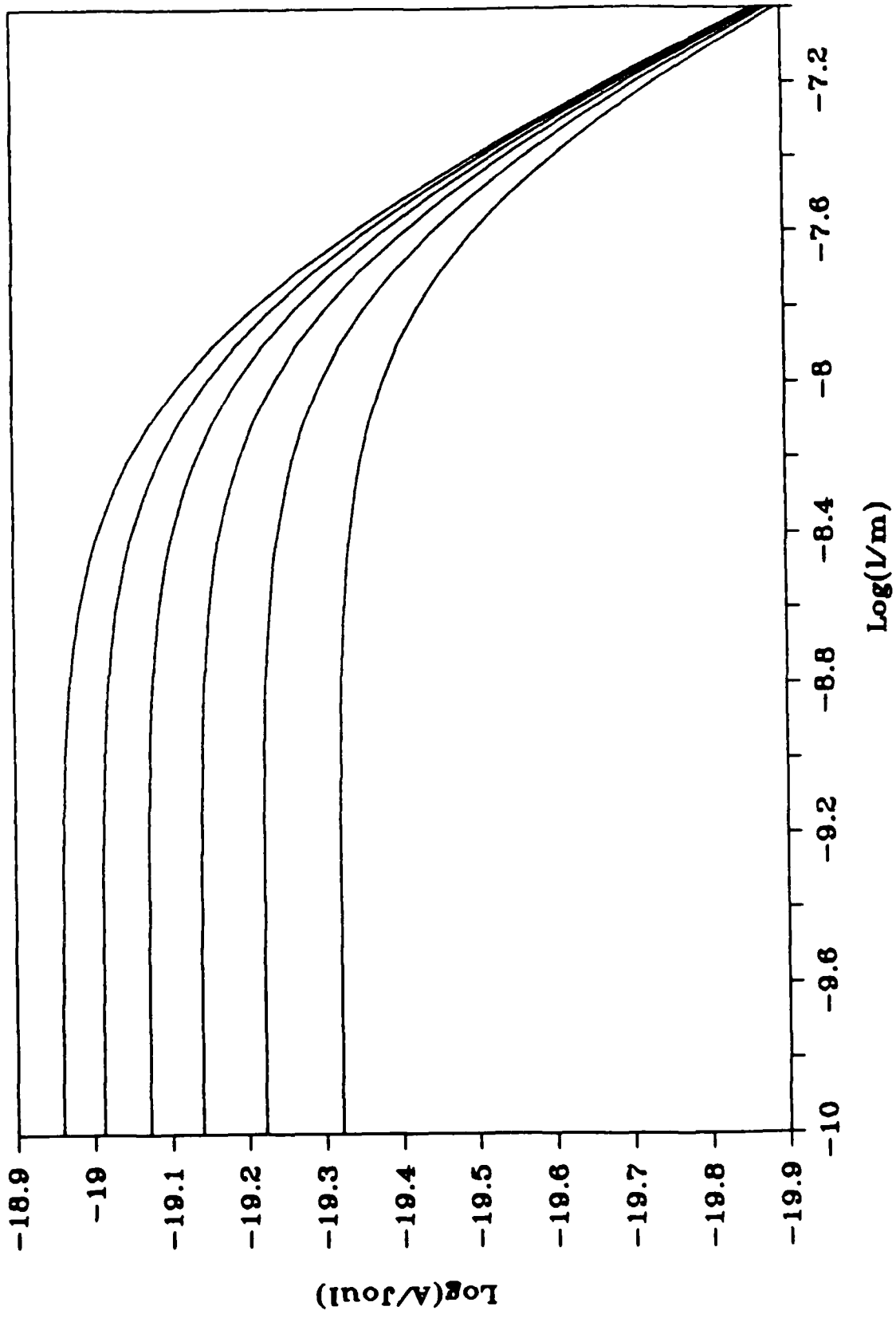
Log(A/Joul)
-18.9
-19
-19.1
-19.2
-19.3
-19.4
-19.5
-19.6
-19.7
-19.8
-19.9
Log(l/m)
-7.2
-7.6
-8
-8.4
-8.8
-9.2
-9.6
-10

Fig. 6

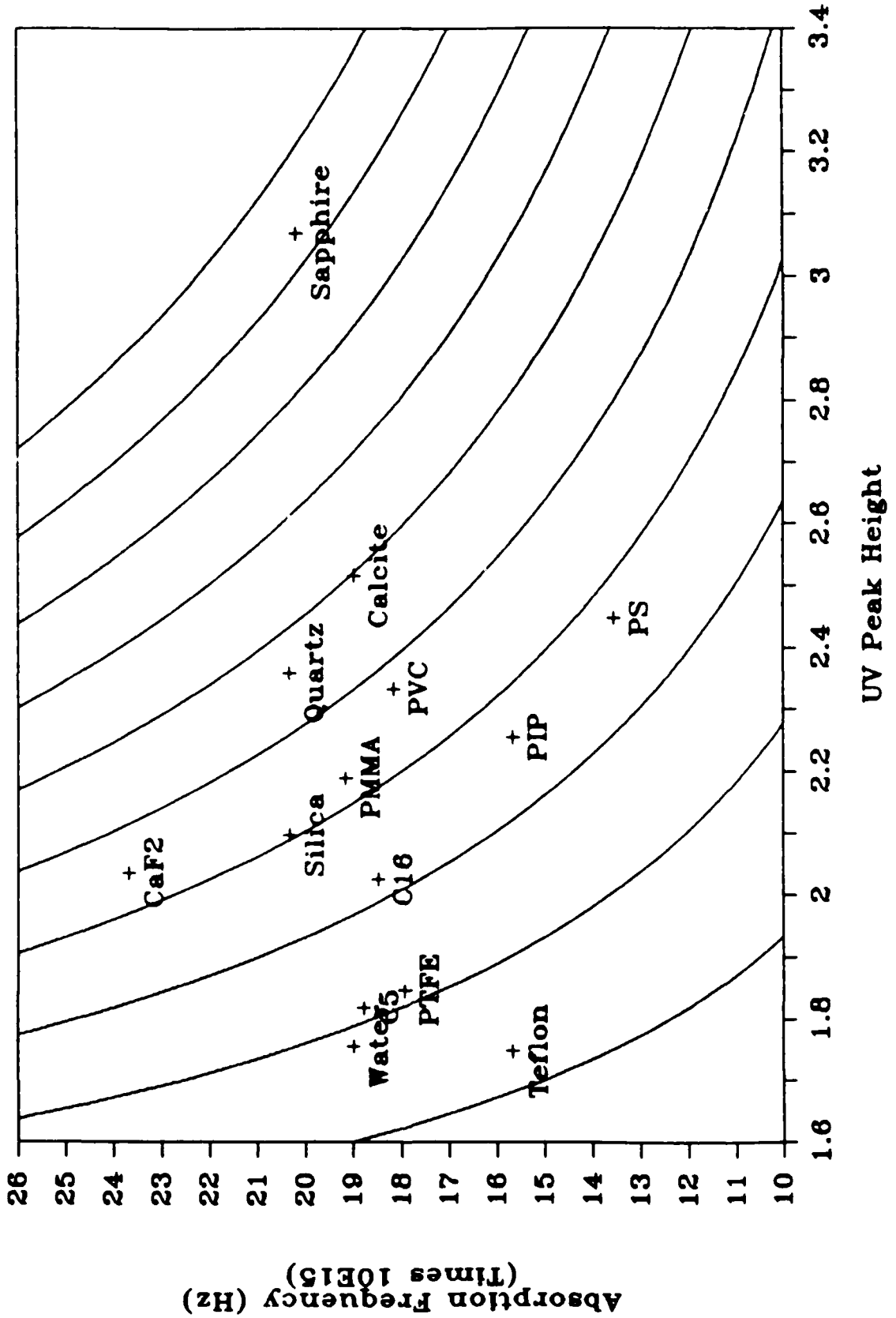
Absorption Frequency (Hz)
(Times 10E15)
26
25
24
23
22
21
20
19
18
17
16
15
14
13
12
11
10
1.6
1.8
2
2.2
2.4
2.6
2.8
3
3.2
3.4
UV Peak Height
Sapphire
Quartz
Calcite
PVC
PS
PMA
PIP
Silica
CaF2
C16
PTFE
Water
Teflon

Fig. 7

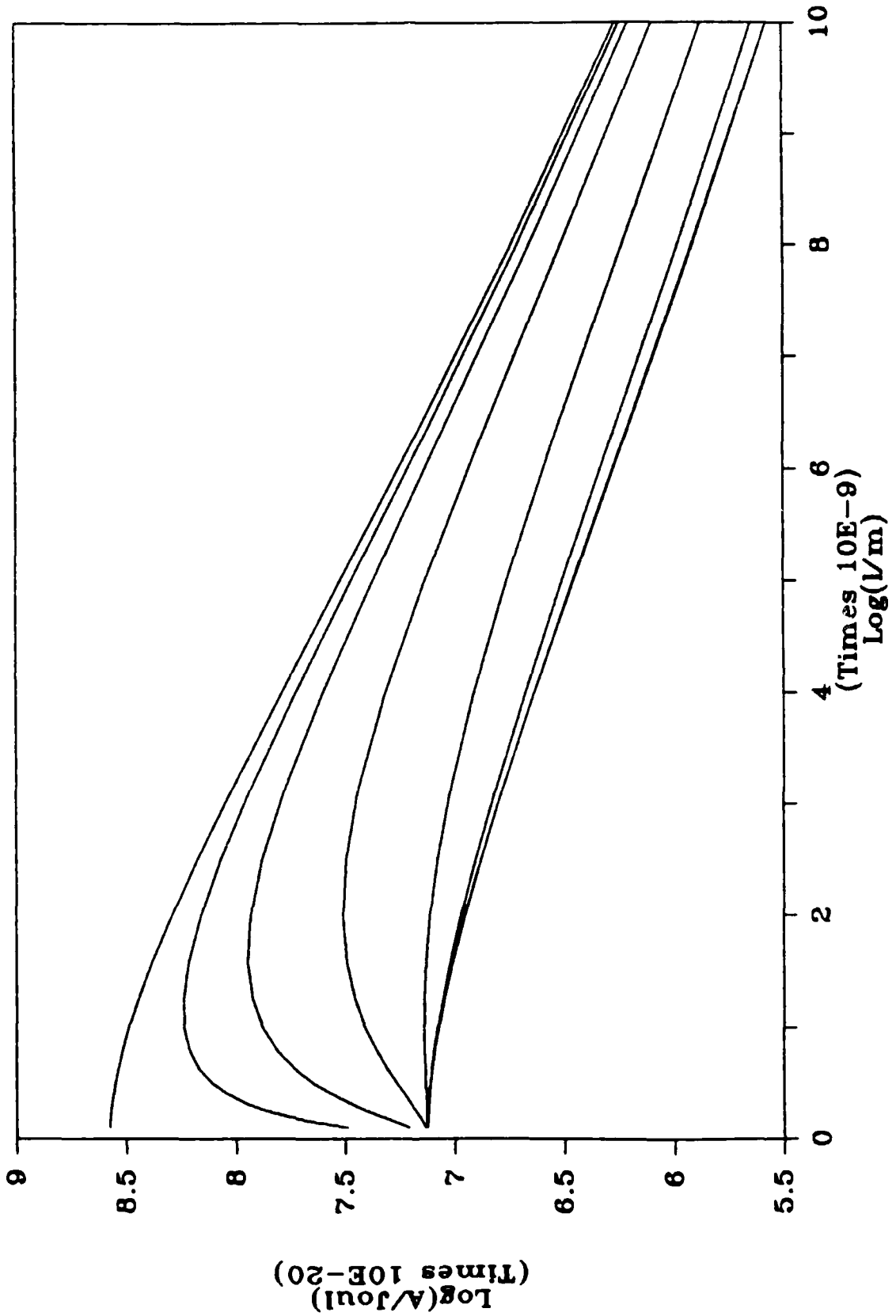
Log(A/Joul)
(Times 10E-20)
9
8.5
8
7.5
7
6.5
6
5.5
0
2
4
6
8
10
(Times 10E-9)
Log(l/m)

Fig. 8

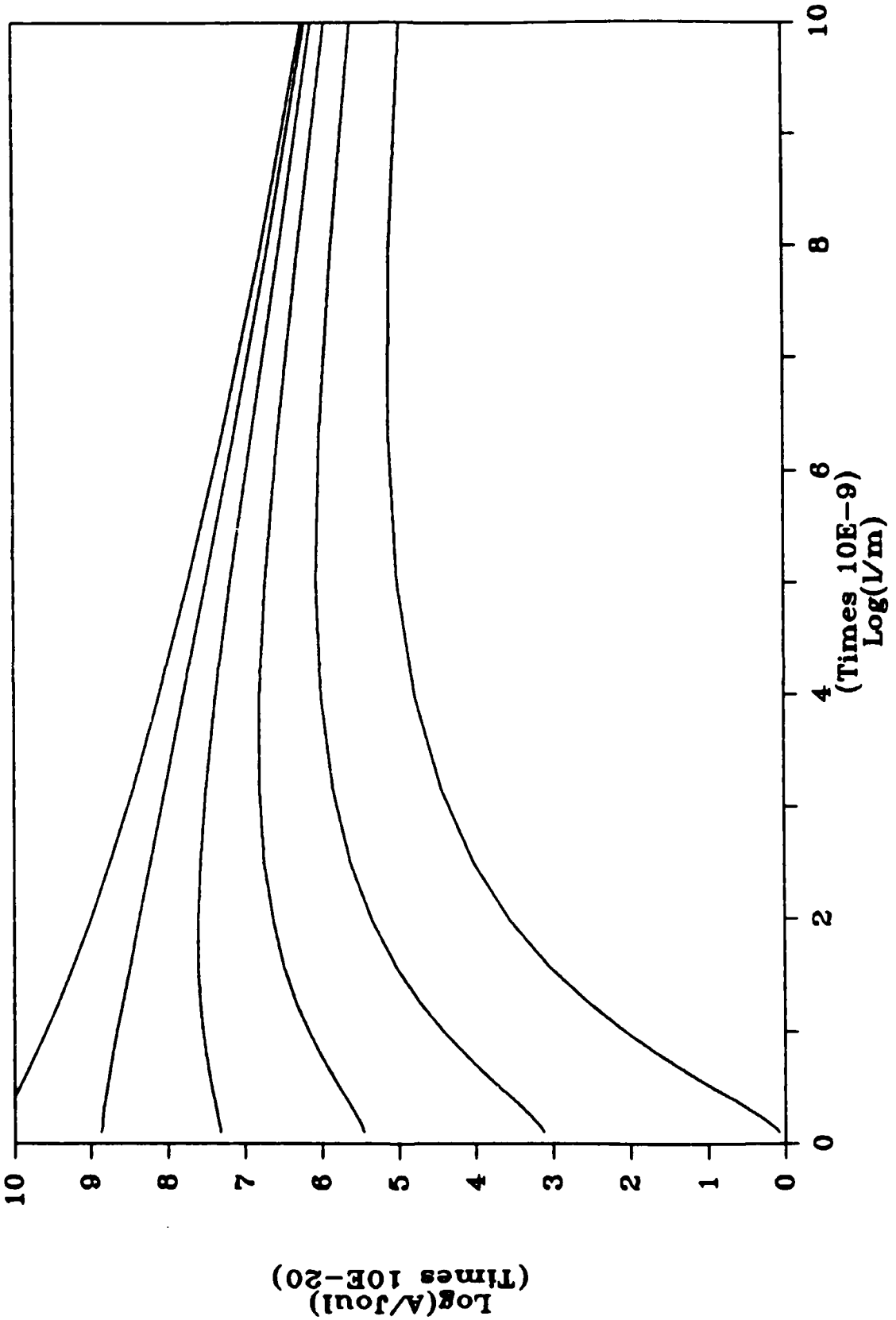
Log(A/Joul)
(Times 10E-20)
10
9
8
7
6
5
4
3
2
1
0
0
2
4
6
8
10
(Times 10E-9)
Log(1/m)

Fig. 9

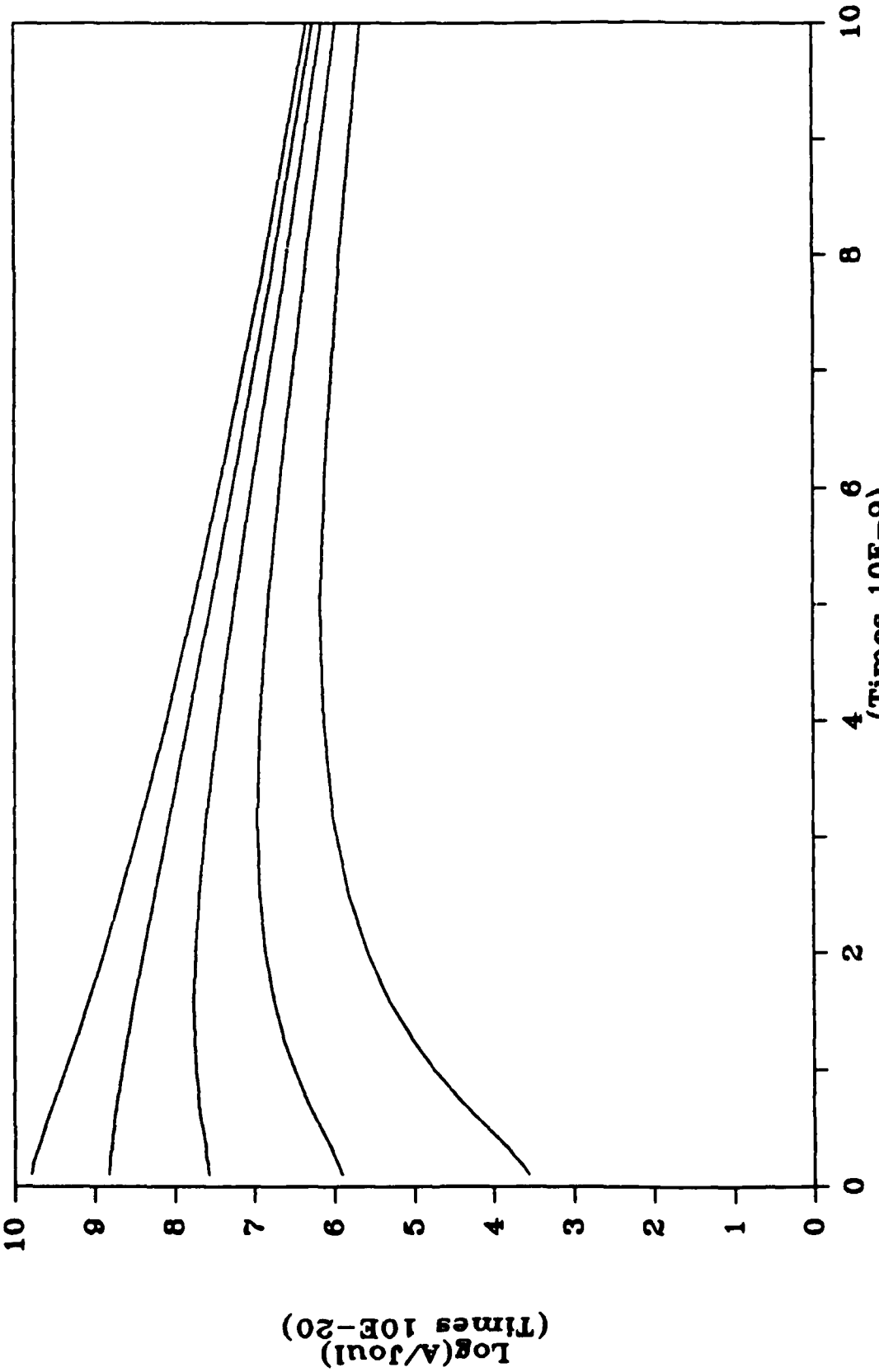
Log(A/Joul)
(Times 10E-20)
10
9
8
7
6
5
4
3
2
1
0
0
2
4
6
8
10
(Times 10E-9)
Log(1/m)

Fig. 10

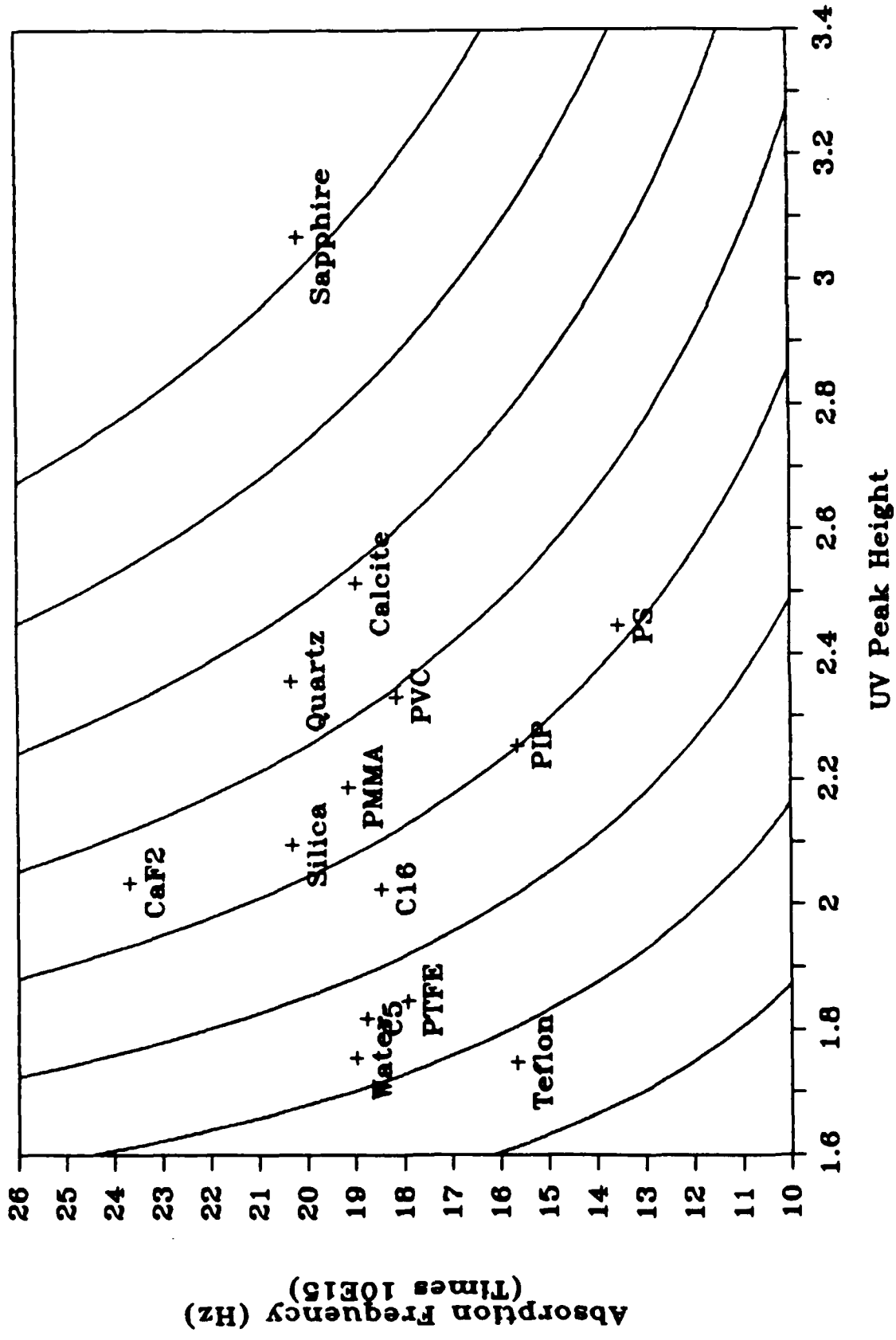
Sapphire
Quartz
Calcite
PVC
PS
PIP
PMMA
Silica
CaF2
C16
PTFE
C5
Water
Teflon
26
25
24
23
22
21
20
19
18
17
16
15
14
13
12
11
10
1.6
1.8
2
2.2
2.4
2.6
2.8
3
3.2
3.4
Absorption Frequency (Hz)
(Times 10E15)
UV Peak Height

Fig. 11

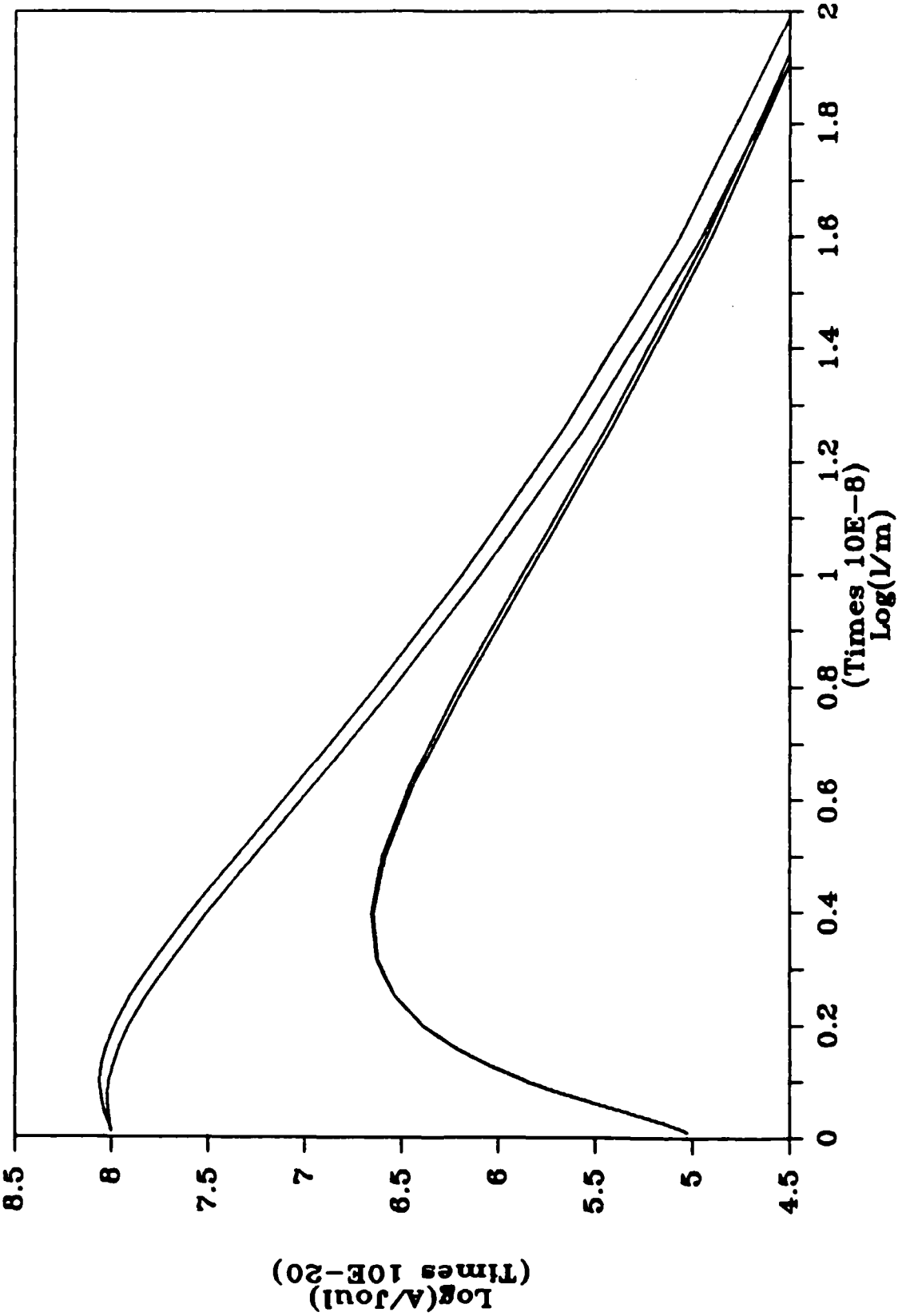
Log(A/Joul)
(Times 10E-20)
8.5
8
7.5
7
6.5
6
5.5
5
4.5
0
0.2
0.4
0.6
0.8
1
1.2
1.4
1.6
1.8
2
Log(l/m)
(Times 10E-8)

Fig. 12

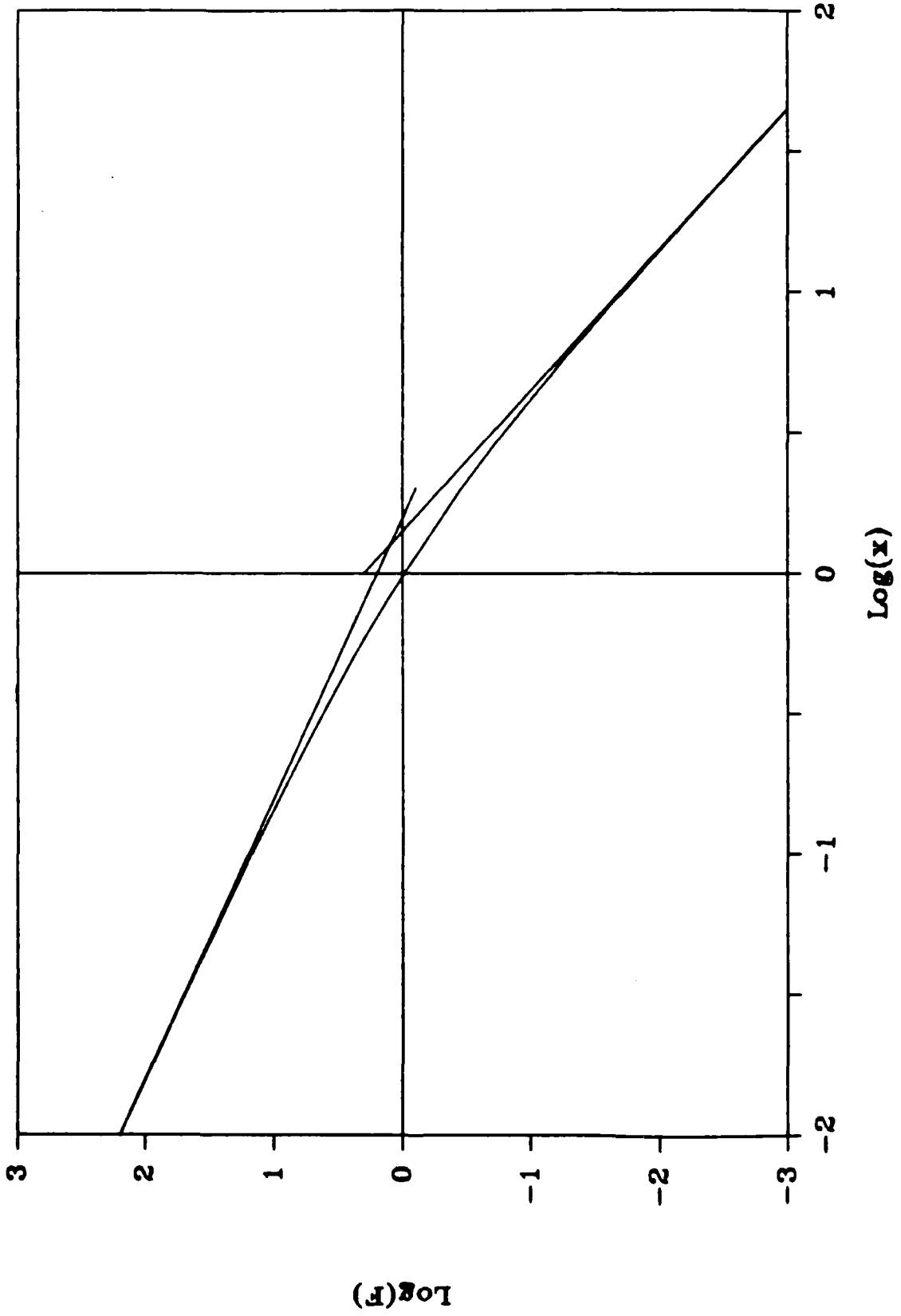

END

DTIC

7-86